ISSN 0001-4338, Izvestiya, Atmospheric and Oceanic Physics, 2022, Vol. 58, No. 9, pp. 1121–1130. © Pleiades Publishing, Ltd., 2022.
Russian Text © The Author(s), 2022, published in Issledovanie Zemli iz Kosmosa, 2022, No. 2, pp. 52–62.

USE OF SPACE INFORMATION ABOUT THE EARTH ENVIRONMENTAL STUDIES BASED ON SPACE DATA

Satellite Assessment of Some Environmental Parameters in the Region of the Iskitim Coal Mines in 2013–2020

N. V. Rodionova*

Kotel'nikov Institute of Radioengineering and Electronics Russian Academy of Sciences, Fryazino Department, Fryazino, Moscow oblast, 141190 Russia

**e-mail: rnv@ire.rssi.ru*

Received July 14, 2021

Abstract—This article discusses the use of multispectral data from Landsat 8, Sentinel 2, Aqua, and Terra satellites for monitoring the environment in areas of open-pit coal mines in the Iskitimsky district of Novosibirsk oblast for 2013–2020. The dynamics of changes in the values of the reflection coefficient (CR) from the surface and water bodies, the snow index NDSI during the snowmelt period, and the change in NDVI in summer are shown. The dynamics of changes in the aerosol optical depth (AOD) (aerosol optical thickness (AOT)) of CO and CH_4 values in the atmosphere of the Iskitimsky district is shown using the Giovanni data analysis and visualization system. A satellite assessment of the state of the atmosphere revealed seasonal changes in the AOD with maximum values in April and July. It is shown that the highest concentrations of carbon monoxide in the atmosphere are observed in the winter months, as well as in the spring of March and April. A stable decrease in the concentration of carbon monoxide in the atmosphere over 7 years from 2014 to 2020 with a determination coefficient of $R^2 = 0.95$ and an increase in the concentration of methane with a determination coefficient of $R^2 = 0.89$ are shown.

Keywords: remote sensing, multispectral data, reflection coefficient, coal mines, surface and atmospheric pollution

DOI: 10.1134/S0001433822090183

INTRODUCTION

Open pit coal mining and its handling and transportation have a negative impact on the environment, polluting the surface and air with emissions of solid substances in the form of coal and inorganic dust, coal ash, and soot. More active coal mining is the cause of man-made earthquakes due to the movement of rocks (https://ngs.ru/text/gorod/2020/09/28/69479455/). Over the past 10 years, the frequency of earthquakes in Novosibirsk oblast has increased; this is directly related to active coal mining. One of the latest earthquakes occurred in September 2020 in the vicinity of the Kolyvansky coal mine (CM) near the village of Ust-Chem.

Satellite images make it possible to estimate the area and degree of pollution of the territories adjacent to coal mining enterprises, mainly for the period of snowmelt.

In this work the satellite monitoring of snow cover pollution in the Iskitimsky district of Novosibirsk oblast near the Kolyvansky and Vostochny coal mines and in the vicinity of the Novosibirsk Electrode Plant in the village of Linevo was carried out using multispectral data from the Landsat 8 (L8) and Sentinel 2 (S2) satellites in order to determine the dynamics of change in the values of CR from the surface, the NDSI snow index during the snowmelt period, and the NDVI vegetation index in the summer for 2013–2020. This paper also evaluates atmospheric pollution based on the use of Terra/Aqua satellite data. The seasonal and interannual variability of AOT, CO, and CH_4 values in the Iskitimsky district is considered using the Giovanni data analysis and visualization system (http://giovanni.gsfc.nasa.gov).

INITIAL DATA AND STUDY AREA

Landsat 8 OLI C2 L2 images with radiometric calibration and atmospheric correction are used as initial images, which can be accessed free of charge, for example, through the EarthExplorer service (https://earthexplorer.usgs.gov). The bands used (B2–B7) of each image were converted from DN brightness values to underlying surface reflectance values. The spatial resolution for multispectral channels is 30 m. Cloudless images of early April (snowmelt) and summer (July–August) 2013–2020 were used.

This work also uses Sentinel 2 multispectral data with high temporal, spatial, and spectral resolution. The multispectral camera has 13 channels with different spatial resolutions from 10 to 60 m. We used data from the S2 survey system with the processing level

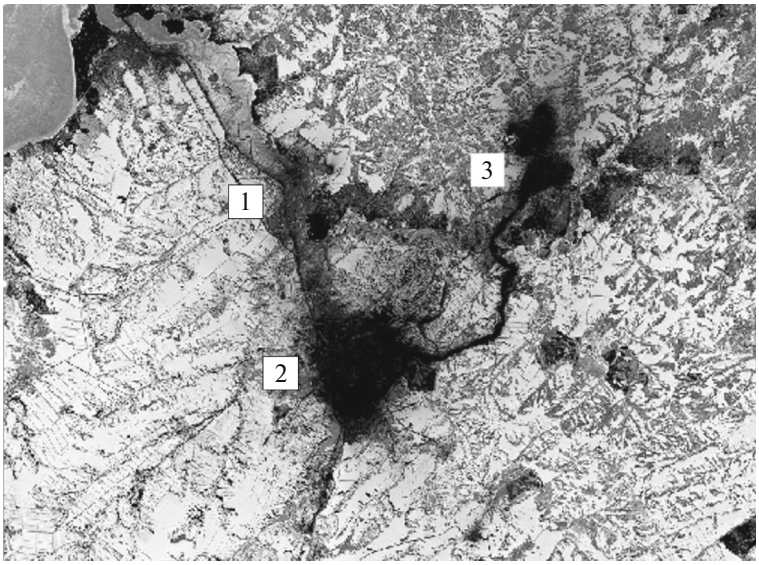

Fig. 1. S2 image of the Iskitimsky district, channel B4, date April 2, 2020.

L2A in the form of albedo at the lower boundary of the atmosphere (with atmospheric correction). S2 data processing was carried out using the SNAP program (https://sentinel.esa.int/web/sentinel/toolboxes/sentinel-1). The S2 images were used when the L8 images were absent or were covered by clouds.

For the analysis of atmospheric pollution, NASA Goddard's Giovanni (http://giovanni.gsfc.nasa.gov) online data visualization and analysis tool was used, which allows a comparison and analysis of large amounts of remote sensing (RS) data (NASA MODIS (Terra and Aqua); ESA MERIS (ENVISAT)) without custom download.

The study area is located in the Iskitimsky district of Novosibirsk oblast (Eastern Siberia). Iskitimsky district is a territory with a high technogenic load. There are several coal basins with open-cast coal mining, an Iskitim Cement Plant, and the Novosibirsk Electrode Plant (Linevo settlement), the raw material base for which are anthracite deposits. All this, as well as all the processes associated with the operation of coal mines, the transportation of coal, leads to negative consequences for the natural environment.

Figure 1 shows the study area on image S2, channel B4, survey date April 2, 2020, with a characteristic type of snow cover pollution in the area of Iskitim (1), Linevo (2), Kolyvansky coal mine and East field of Kolyvansky deposit (3), Urgunsky, and Gorlovsky coal mines and highways through which coal is transported. A fragment of the Ob Reservoir is visible in the upper left part of the image.

SATELLITE ENVIRONMENTAL ASSESSMENT

The work (Purkis and Klemas, 2011) shows that the minimum time interval for studying the technogenic impact of mining on the environment is 5 years.

Monitoring Snow Cover during the Snowmelt Period

To assess the level of surface pollution in the winter–spring period, an assessment of snow cover pollution during the snowmelt period is used. Snow cover, which has a cumulative effect, makes it possible to obtain the real total value of pollutant fallout (P). The evaluation criterion is the reflective characteristics of the snow cover in various spectral channels and snow indices, one of which is the NDSI index (Normalized Difference Snow Index) (Hall et al., 1995), defined as NDSI = (GREEN – SWIR1)/(GREEN + SWIR1). The threshold for snow identification is NDSI ≥ 0.4 (Hall et al., 1995).

Let us compare the reflection coefficient (CR) from the snow cover and the NDSI values near the Kolyvansky coal mine (Fig. 1 (3)) and the settlement of Linevo (Fig. 1, (2)) in 2013 and 2020.

The territory of coal mines in the area of the Kolyvansky coal mine increased from 2013 to 2020 (Fig. 2).

Figure 3 shows graphs of changes in the reflectivity and NDSI values along the profile in the region of the Kolyvansky and Vostochny coal mines during the snowmelt period for April 9, 2013 (L8) (Fig. 3, top row) and April 2, 2020 (S2) (Fig. 3, bottom row). The profile consists of 14 points. The abscissa shows the distance in km from the "zero point" (the value 0 km corresponds to the point with coordinates 54°39′47″ N and 83°37′30″ E near the road to the coal mine). The NDSI value for all points of the 2013 profile is greater than 0.5; snow was identified at these points. For 2020, snow was not identified for profile points up to 2.5 km in the direction towards the village of Ust-Chem (from the 0 point) and about 1.2 km (from the 0 point) westward.

Snow pollution near the village of Linevo is associated with the work of the Novosibirsk Electrode

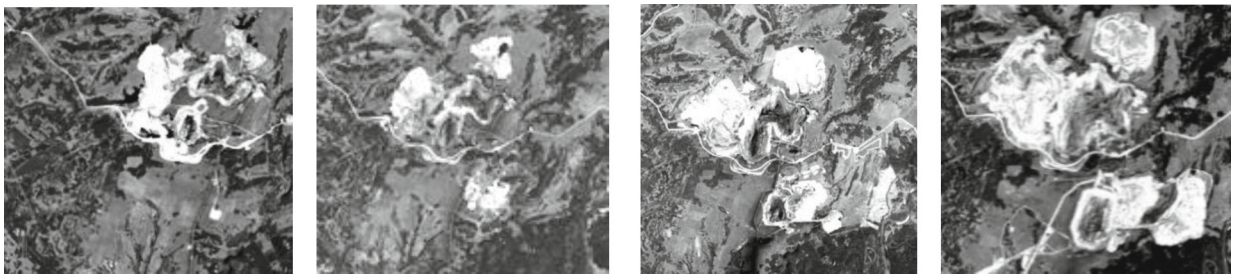

Fig. 2. Dynamics of changes in the territories of the Kolyvansky and Vostochny coal mines from 2013 to 2020 according to L8.

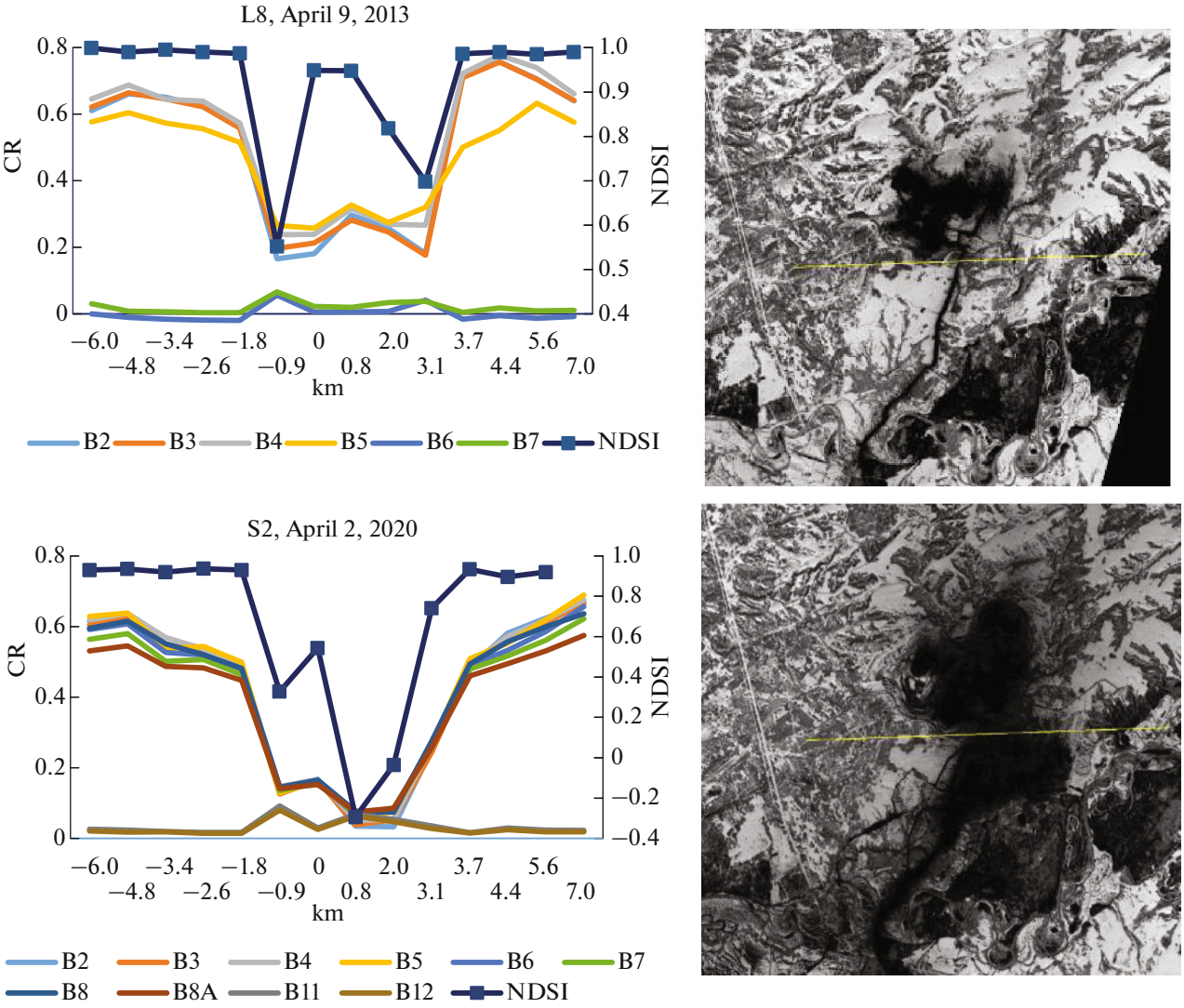

Fig. 3. Graphs of changes in CR and NDSI for the profile in the region of the Kolyvansky and Vostochny coal mines for April 2013 and 2020.

Plant (NEP). Dust emissions from NEP high-altitude chimneys, coal processing plants, quarrying, and the technological route in the vicinity of the NEP are the main sources of pollution in the area of Linevo settlement. Figure 4 shows graphs of changes in CR and NDSI for April 9, 2013 (L8) (top row) and April 2, 2020 (S2) (bottom row), along an 8-point profile passing through Linevo. The abscissa shows the distance in km from the "zero kilometer" (the value of 0 km corresponds to the point with coordinates 54°31′15″ N

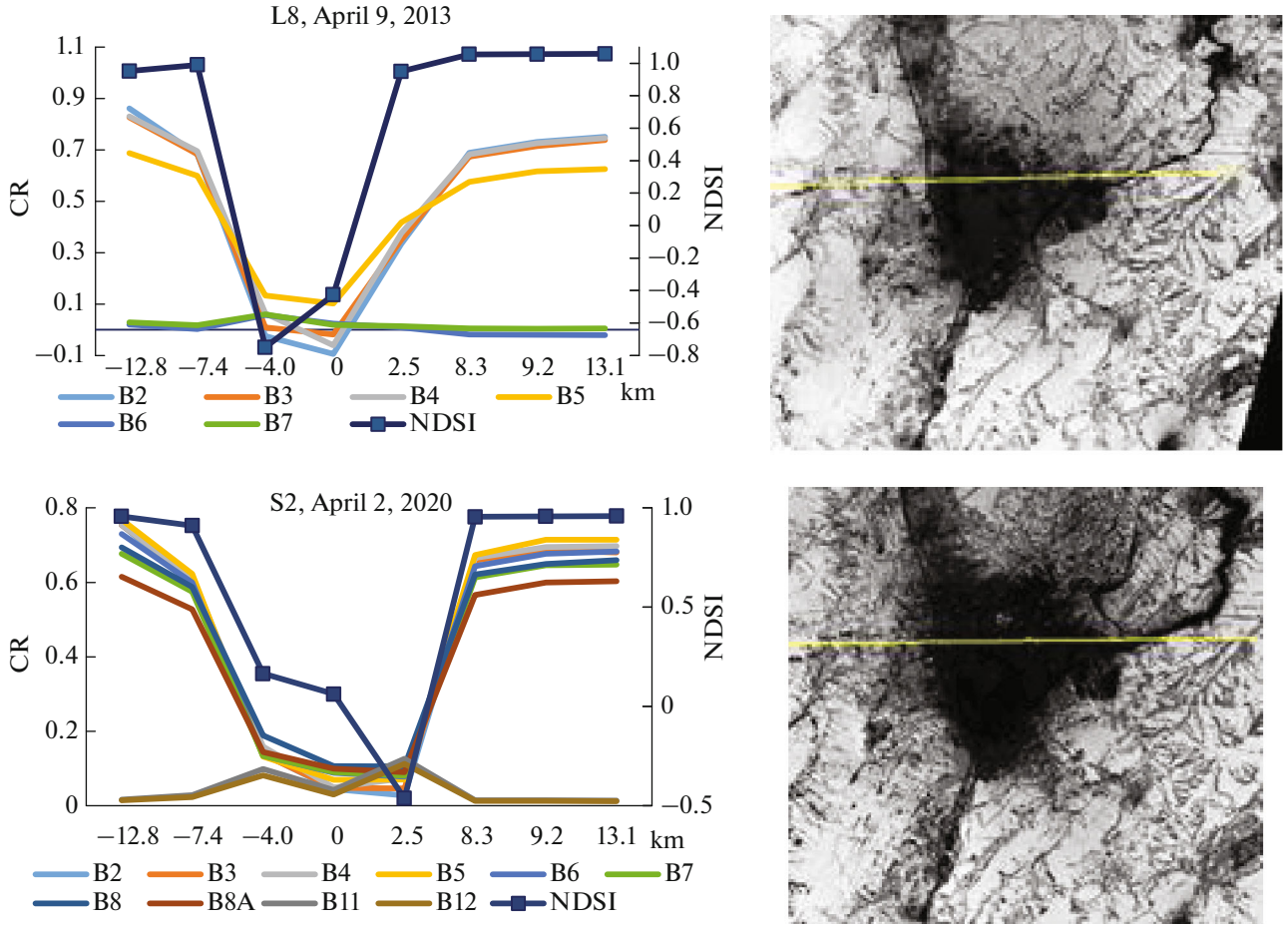

Fig. 4. Graphs of changes in CR and NDSI for the profile in the Linevo settlement region for April 2013 and 2020.

and 83°24′05″ E, near the NEP). The snow-free zone in 2020 relative to 2013 remained virtually unchanged westward from the zero point, while at the same time it expanded eastward by 4–5 km.

Monitoring NDVI Changes

To assess the state of vegetation, integral characteristics are used, expressed in the form of vegetation indices (VI). The basis for choosing VI is the features of the vegetation reflectivity curves, namely, in the red region of the spectrum (RED) there is a maximum absorption of solar radiation by chlorophyll; in the near infrared (NIR) there is a maximum reflection of energy by the cellular structure of the leaf. As a result, the normalized difference index NDVI = (NIR – RED)/(NIR + RED) is most commonly used to quantify phytomass density.

Technogenic factors associated with open pit coal mining have a negative impact on the vegetation cover. Pollution of the atmosphere, soil, water environment, etc., are factors that disrupt the growth and development of vegetation.

In this paper we compared the values of CR and NDVI for the profile in Linevo settlement according to L8 data for the summer period for the dates July 30, 2013, and August 2, 2020 (the profile is the same as in Fig. 4).

We note in Fig. 5 the local minimum of CR values at the point of "zero" km (near the NEP). The NDVI values for all profile points, except for the 9.2 km point, for 2013 exceed the NDVI values for 2020.

Figure 6 shows the RGB images of the study area for the summer period, demonstrating the dynamics of changes in the values of NDVI = (B5 – B4)/(B5 + B4) (channels L8). Survey dates July 30, 2013; August 4, 2018; and August 2, 2020, have the following coding of NDVI values: red, NDVI < 0.4; green, NDVI > 0.7; and deep blue, (NDVI ≥ 0.4) and (NDVI ≤ 0.7). There is a tendency from 2013 to 2020 for an increase in territories with NDVI values < 0.7.

Monitoring Changes in the Reflection Coefficient from Water Bodies

Figure 7 shows the Landsat 8 image (B5, August 2, 2020) on which the water bodies that are the subject of

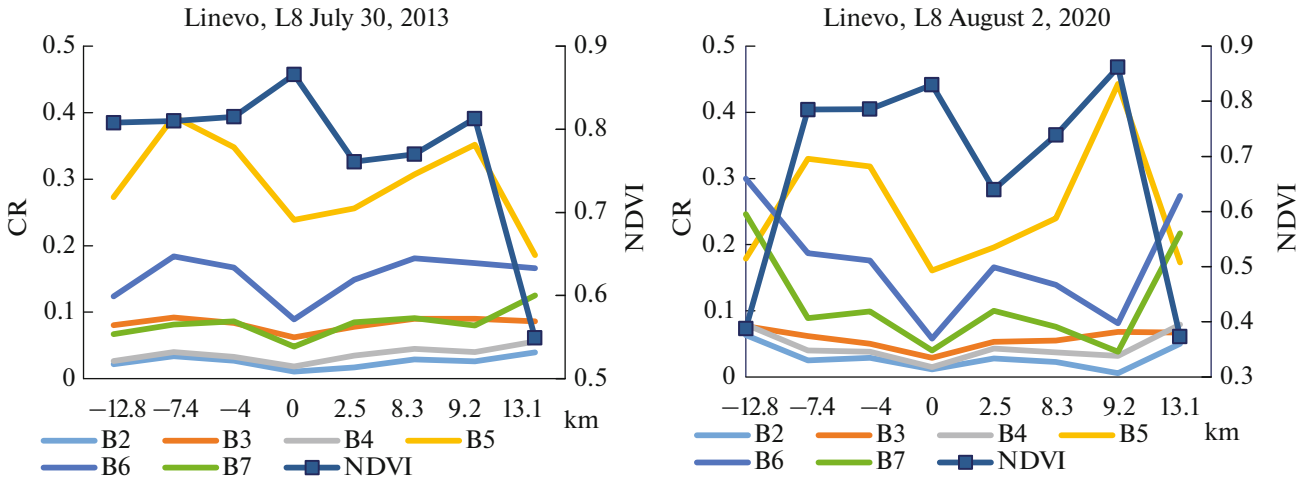

Fig. 5. Graphs of changes in CR and NDVI for the profile in the settlement of Linevo according to L8 data.

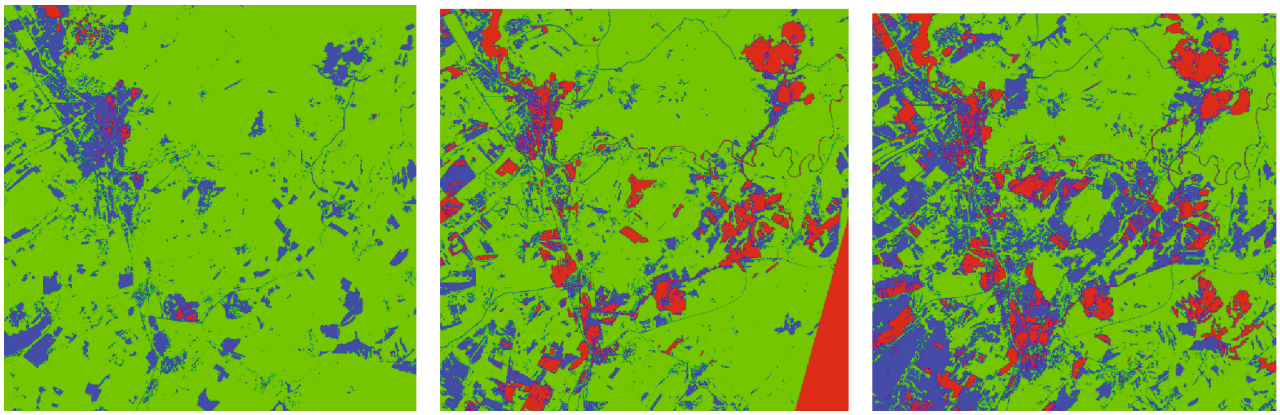

Fig. 6. RGB maps of NDVI values for July 30, 2013; August 4, 2018; and August 2, 2020.

monitoring in this work are marked with numbers: the Ob Reservoir (1), the Berd' River at the bridge (2), the Berd' River (3), Lake Linevo (4), and Lake Koinikha (5). Spectral curves for the wavelengths of channels B2–B7 are shown in Fig. 8 for four dates July 30, 2013; July 8, 2014; July 31, 2019; and August 2, 2020.

It was shown in (Oparin et al., 2014) that the two spectral bands NIR and SWIR are very sensitive to the presence of impurities in the aquatic environment. In closed reservoirs (Lake Linevo), such impurities settle to the bottom, while for reservoirs with active water flow, the particles are mixed, which causes a jump in CR values. In addition, the presence of suspended particles in the aquatic environment increases CR in the NIR spectrum and organic matter in SWIR1. On the graphs of Fig. 8 for 2013, we observe two peaks of CR values: in the green region of the spectrum B3 and in NIR (B5). The first maximum is present on the charts for other dates as well. The increase in CR in channel B3 is associated with an increase in the volume of phytoplankton. The decrease in CR in the red

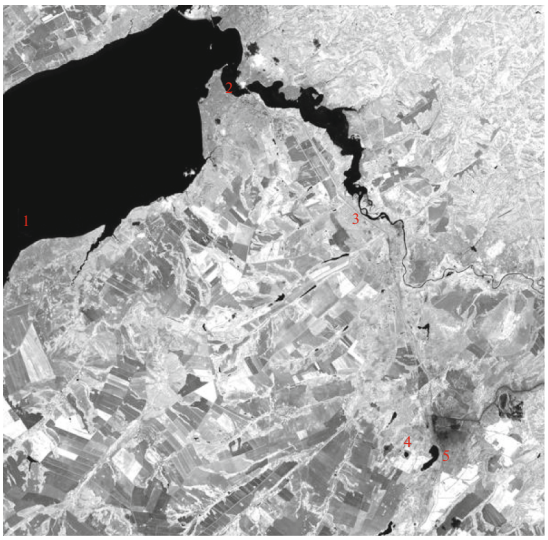

Fig. 7. Water bodies under consideration in image L8, survey date August 2, 2020: (1) Ob Reservoir, (2) Berd' River near the bridge, (3) Berd' River, (4) Lake Linevo, and (5) Lake Koinikha (L8, B5 channel, August 2, 2020).

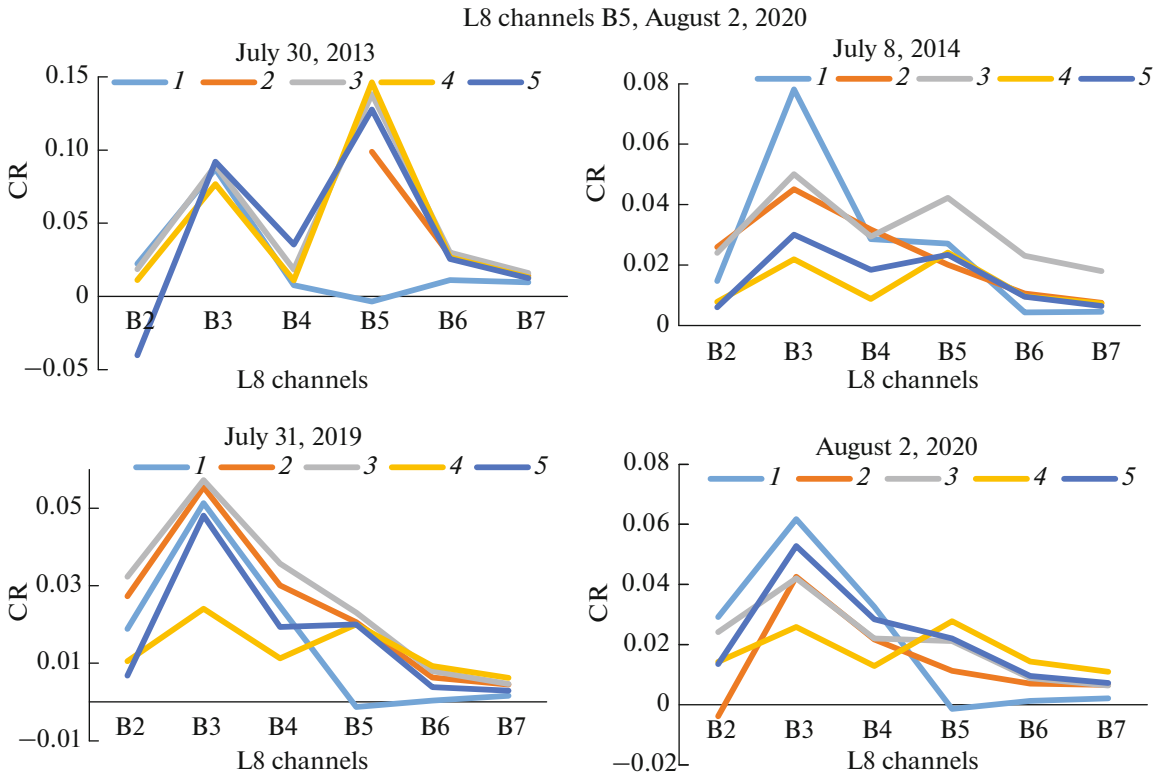

Fig. 8. Spectral curves for water bodies: (*1*) Ob Reservoir, (*2*) Berd' River near the bridge, (*3*) Berd' River, (*4*) Lake Linevo, and (*5*) Lake Koinikha.

zone of the spectrum is associated with the absorption of chlorophyll by plankton and, consequently, a decrease in CR in the B4 channel. The smallest variations in channels B2–B7 are characteristic of object 4—Lake Linevo (except for 2013). The second maximum (channel B5) is associated with the presence of suspended impurities in the aquatic environment. In 2013, the CR value for B5 is three or more times higher than the CR value for 2014–2020. The exception is the CR value for the Ob Reservoir, for which the CR values in channel B5 are the lowest in comparison with other water bodies. The second maximum, pronounced in 2013, has been gradually disappearing since 2014, and the CR values gradually decrease when moving from the B5 channel to the B7 channel.

Satellite-Based Atmospheric Assessment

Iskitim is a city with a high level of air pollution (AP). The substances that determine the level of AP in Iskitim are benz(a)pyrene, suspended matters (dust), CO (carbon monoxide), NO_2/NO (nitrogen dioxide/oxide), SO_2 (sulfur dioxide), hydrogen sulfide, and soot. Iskitim is located in a lowland, which contributes to the accumulation of harmful substances in the air above the city.

This paper examines the dynamics of changes for 2013–2020 of aerosol optical depth (AOD) (aerosol optical thickness (AOT)), CO, and CH_4 values in the Iskitim region using the Giovanni data analysis and visualization system (http://giovanni.gsfc.nasa.gov).

Seasonal and Interannual Variations in the AOT of the Atmosphere

Among the radiation-significant components of the atmosphere, along with greenhouse gases and clouds, an important role is played by atmospheric aerosol, the main optical characteristic of which is the AOD of the atmosphere. Aerosol particles have a significant impact on the temperature balance of the atmosphere, because they are able to absorb, scatter, and reflect the solar radiation and initiate cloud formation processes. The main natural factors affecting the long-term variability of AOT are volcanic eruptions (Bryson and Goodman, 1980) and forest fires (Sakerin et al., 2008). During open-cast coal mining, the main pollutants are solid emissions: inorganic dust, coal dust, coal ash, and soot. To analyze spatio-temporal variations in AOD, the data of satellite measurements, in particular, the MODIS radiometer of the Terra/Aqua satellites, are increasingly used.

To estimate atmospheric aerosol variations, we used level 3 (daily average) data from the MODIS radiometer collection 6.1 (Terra satellite) – Terra MOD08_D3 v6 product. 1 (Deep Blue, Land only) at

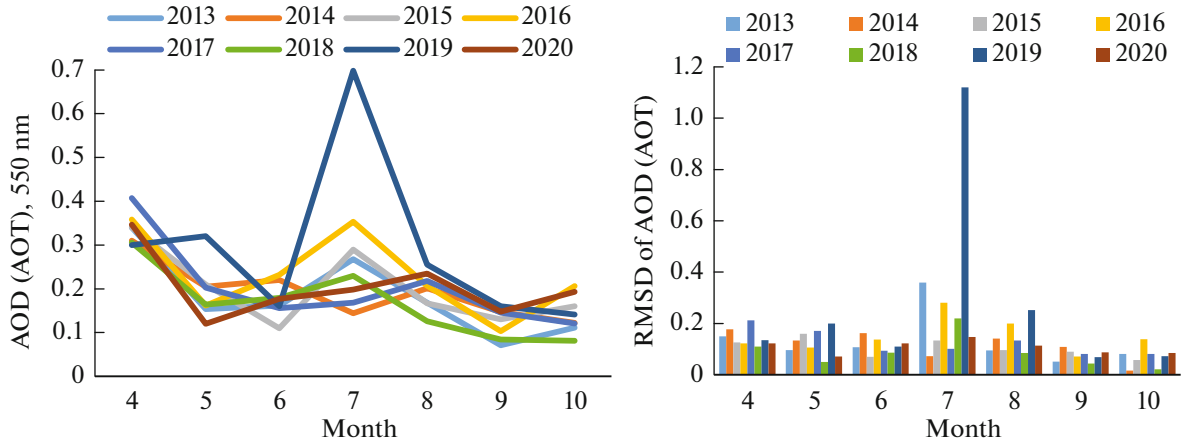

Fig. 9. Average values of AOD (AOT) and RMSD of AOD (AOT) for April to October 2013–2020 for the study area according to MODIS data (Terra).

550 nm. AOD data obtained with MODIS is a 2D field (image) integrated over height. The dimensions of individual elements (pixels) of the map are 1° × 1° (latitude *x* longitude). Monthly mean AOD values were calculated for the period April to October 2013–2020, averaged for the area 1° × 1° with a center coordinates 54.5° N and 83.5° E using the Giovanni data analysis and visualization system.

Figure 9 shows the seasonal course of AOD values for April to October 2013–2020 and AOT RMSD.

We note the seasonal course of the AOT with a maximum in the spring–summer period (April and July) and a minimum in autumn (data for the winter period are not available). Similar trends are also observed for the Baikal Region (Tashchilin et al., 2021). In July, the increase in AOT values was most noticeable in 2019. It should also be noted that there was a significant spread in AOT values in July 2019. One of the main reasons for the April AOD maximum in the Iskitimsky district is the release of aerosol during the snowmelt, accumulated in the snow cover in winter. The local minimum in May may be associated with the formation of fresh vegetation and an increase in the level of precipitation, which washes out the aerosol. The AOD maximum in July is most likely associated with an increase in temperature, a decrease in humidity, and drought.

Figure 10 shows a plot of interannual AOT variations for the period 2013–2020. No annual trend was found. Large fluctuations in interannual AOD values are observed. For 2018, the average annual AOD value is close to the annual average global value of 0.16 obtained from MODIS, TOMS, and AVHRR satellite data (Chubarova et al., 2012). For other dates for the Iskitimsky district, the average annual AOD values significantly exceed the annual average global value and the value for the Baikal Region (MODIS data and ground-based measurements of solar photometers, (Tashchilin et al., 2021)).

Seasonal and Interannual CO Variations

The main sources of CO are the combustion of fossil fuels, biomass, and the atmospheric oxidation of methane and other hydrocarbons. Carbon monoxide is a colorless and odorless gas. CO is formed during the combustion of fossil fuels (wood, coal, paper, oils, gasoline, etc.). The predominant part (~90%) of atmospheric CO is formed as a result of natural processes (volcanic and swamp gases, forest and steppe fires, and the vital activity of terrestrial and oceanic flora and fauna). At the same time, about 70% of CO in the atmosphere is a product of methane oxidation in the troposphere with the participation of the hydroxyl (OH) radical. On a global scale, it is an atmospheric methane (which is oxidized by OH) that is the main source of CO in the atmosphere. In large cities and industrial regions, the predominance may be on the side of CO directly emitted from the anthropogenic sources. Hundreds of millions of tons of CO annually enter the atmosphere as a result of human activities: motor

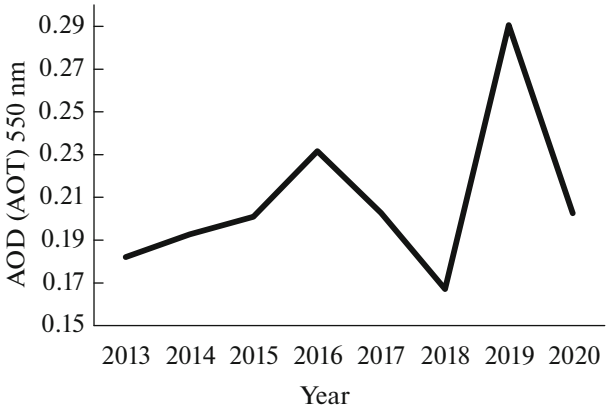

Fig. 10. Interannual variations in AOD (AOT) for the period 2013–2020.

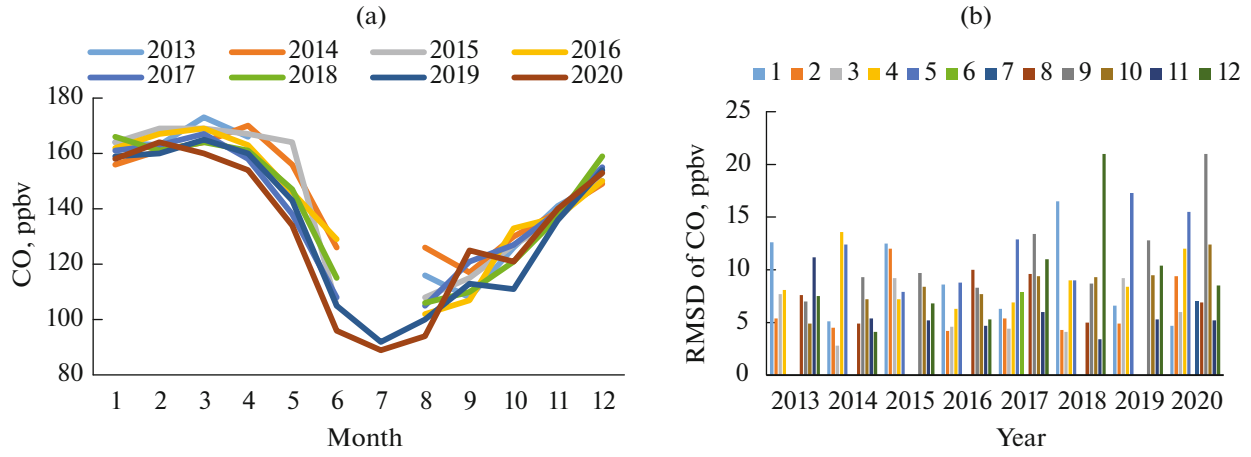

Fig. 11. Average monthly changes in carbon monoxide concentration, averaged for the area 54°–55° N, 83°–84° E.

transport; rail and sea transport; malfunctions of gas pipelines and gas equipment; metallurgy, chemical industry, coal mining, tobacco, bread production, and light industry; waste processing; and home fuel combustion. In industry, CO is formed as a result of the incomplete oxidation of natural gas or the gasification of coal and coke. CO enters the atmospheric air during any type of combustion. In cities, CO enters the air mainly as part of the exhaust gases of internal combustion engines. CO has a long lifetime, about a month (Deryugina, 2017).

To study variations of atmospheric CO content, daily (day time) data from the AIRS/Aqua product (AIRS3STM v006 product) averaged over the region 54°–55°, 83°–84° E were used. Figure 11a shows the average monthly values of CO concentration, and Fig. 11b shows the RMSD values of CO for the period 2013–2020. Characteristic in the behavior of the graphs for all 8 years from 2013 to 2020 is (1) the highest concentrations of CO in the winter months, as well as in the spring months—March and April; (2) the lowest concentrations of CO in the summer months.

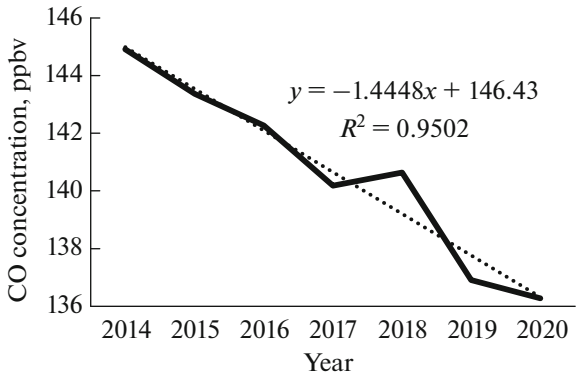

Fig. 12. Average annual values of CO concentration for 2014–2020 with a trend line.

Figure 12 shows the average annual concentrations of CO for 2014–2020. Averaging was carried out over 11 months (the month of July not included due to a lack of data for 2013–2018). The graph does not include data for 2013 because, apart from July, there is no data for May for this year. The trend line with the determination coefficient $R^2 = 0.95$ indicates a stable decrease in CO concentration over 7 years from 2014 to 2020. In 2014, the average annual CO concentration was 0.145 ppm = 0.168 mg m^{-3}. The annual average for 2020 is 0.136 ppm = 0.158 mg m^{-3}. The average daily MPC (maximum permissible concentration) of CO equals MPCad = 0.05 mg m^{-3}, and the maximum one-time MPCmt = 0.15 mg m^{-3} (https://vozdyx.ru/article/pdk-vrednyx-veshhestv-v-atmosfernom-vozduxe/).

Seasonal and Interannual Variations in CH_4

Methane enters the atmosphere as a result of both natural and anthropogenic processes. Wetlands are the main natural source of methane emissions into the atmosphere. Methane is formed mainly as a result of the activity of bacteria involved in the decomposition of organic matter. Therefore, the main places of methane formation are swamps, garbage dumps, etc. In addition, methane is released through cracks in the Earth's crust at the bottom of water bodies, during mining, and during forest fires. Anthropogenic sources of methane in the atmosphere are energy production from coal and natural gas, landfills, sewage treatment plants, agriculture (manure processing), rice growing, and biomass burning. Methane is emitted during the production and transportation of coal, natural gas, and oil. Once released, methane remains in the atmosphere for about 10 years, after which it is removed primarily by chemical oxidation in the troposphere. The main mechanism for removing methane from the atmosphere is its oxidation in the upper

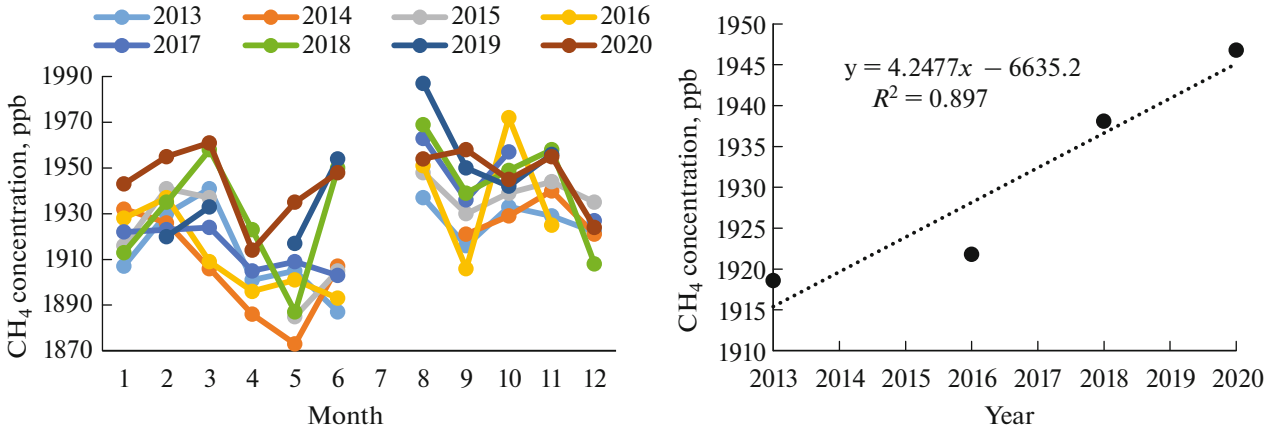

Fig. 13. Seasonal and interannual variations in methane concentration for 2013–2020.

atmosphere by the hydroxyl radical OH, which is formed under the influence of sunlight from ozone and water vapor.

Figure 13 shows graphs of seasonal and interannual variations in CH_4 concentration values based on monthly (day time) data from the AIRS (Atmospheric Infrared Sounder) infrared spectrometer installed on the EOS AQUA satellite (AIRS3STM v.7.0 product). These are maps of methane distributions with a resolution of 1° × 1° at a pressure altitude of 1000 hPa, available at the link (http://giovanni.gsfc.nasa.gov). The product has a data pass for the month of July.

According to Fig. 13, the local methane concentration maxima were observed in March, August, and October. A decrease in values was noted in April–May and in the winter months. The mean RMSD value is about 31 ppb. It is known that the average concentration of CH_4 in the atmosphere is 1.86 ppm (Repina, 2015). The concentration of methane over the study area exceeds the average value for the atmosphere. The graph of interannual values of CH_4 concentration was built by averaging the values for 10 months (January–June, August–November). The trend line with the determination coefficient $R^2 = 0.89$ indicates a steady increase in methane concentration over the period 2013–2020.

CONCLUSIONS

According to satellite monitoring data of the Iskitimsky district with a high technogenic load for the period 2013–2020, the following changes have been outlined in the ecology of the region. The zone of dirty snow expanded eastward by 3–5 km in the Linevo region and in the region of the Kolyvansky and Vostochny coal mines during that period. The dynamics of the decrease in the values of the vegetation index NDVI is shown. The seasonal variation of AOD is shown with maximum values in April and July. In 2018, the average AOD is close to the annual global average of 0.16. For other dates for the Iskitimsky district, the average annual AOT is significantly higher than the average annual global value. It is shown that the highest concentrations of carbon monoxide in the atmosphere are observed in the winter months, as well as in the spring months of March and April. The summer months are characterized by the lowest CO concentrations. A stable decrease in the concentration of carbon monoxide in the atmosphere over 7 years from 2014 to 2020 with a determination coefficient of $R^2 = 0.95$ and an increase in the concentration of methane with a determination coefficient $R^2 = 0.89$ are shown.

FUNDING

This work was carried out as part of the State Task of the Kotel'nikov Institute of Radioengineering and Electronics of the Russian Academy of Sciences, Fryazino Department, on the topic 0030-2019-0008 Space.

CONFLICT OF INTERESTS

The author declares that she has no conflicts of interest.

REFERENCES

Bryson, R.A. and Goodman, B.M., Volcanic activity and climatic changes, *Science*, 1980, vol. 207, pp. 1041–1044.

Chubarova, N., Nezval, Ye., Sviridenkov, M., Smirnov, A., and Slutsker, I., Smoke aerosol and its radiative effects during extreme fire event over central Russia in summer 2010, *Atmos. Meas. Tech.*, 2012, vol. 5, pp. 557–568.

Deryugina, A.B., Analysis of local measurements of CO concentrations in Peterhof, St. Petersburg: Russian State Hydrometeorological University, 2017. http://elib.rshu.ru/files_books/pdf/rid_8cfe04d7c0304f5587627e49f20d451a.PDF.

Hall, D.K., Riggs, G.A., and Salomonson, V.V., Development of methods for mapping global snow cover using moderate resolution imaging spectroradiometer

(MODIS) data, *Remote Sens. Environ.*, 1995, vol. 54, no. 2, pp. 127–140.

Oparin, V.N., Potapov, V.P., and Giniyatullina, O.L., Integrated assessment of the environmental state from remote sensing of the Earth in regions with high anthropogenic load, *Fiz.-Tekh. Probl. Razrab. Polezn. Iskop.*, 2014, no. 6, pp. 199–209.

Purkis, S. and Klemas, V., *Remote Sensing and Global Environmental Change*, Wiley-Blackwell, 2011.

Repina, I., Remote investigations of methane concentrations and fluxes in the atmosphere, 2015. http://d33.infospace.ru/d33_conf/tarusa2015/07.pdf.

Sakerin, S.M., Gorbarenko, E.V., and Kabanov, D.M., Features of long-term variability of aerosol optical thickness in the atmosphere and estimates for the impact of different factors, *Opt. Atmos. Okeana*, 2008, vol. 21, no. 7, pp. 625–631.

Tashchilin, M.A., Yakovleva, I.P., and Sakerin, S.M., Spatiotemporal variations in aerosol optical thickness in the Baikal region, *Sovrem. Probl. Distantsionnogo Zondirovaniya Zemli Kosmosa*, 2021, vol. 18, no. 1, pp. 219–226.

Translated by V. Selikhanovich